JOURNAL OF BIOMEDICAL OPTICS 1(4), 455–465 (OCTOBER 1996)

INFRARED RADIOMETRY OF DENTAL ENAMEL DURING ER:YAG AND ER:YSGG LASER IRRADIATION

Daniel Fried,[†] Steven R. Visuri,[‡] John D. B. Featherstone,[†] Joseph T. Walsh,[*] Wolf Seka,[**] Richard E. Glena,[***] Sandra M. McCormack,[***] and Harvey A. Wigdor[§]

[†]University of California, San Francisco, Biomaterials Science Division, Department of Restorative Dentistry, Box 0758, San Francisco, California 94143; [‡]Lawrence Livermore National Laboratory, Livermore, California 94551; [*]Northwestern University, Biomedical Engineering Department, Evanston, Illinois 60208-3107; [**]University of Rochester, Laboratory for Laser Energetics, Rochester, New York 14623; [***]Eastman Dental Center, Rochester, New York 14620; [§]Ravenswood Hospital Medical Center, Wenske Laser Center, Chicago, Illinois 60660

(Paper JBO-087 received Apr. 15, 1996; revised manuscript received Aug. 12, 1996; accepted for publication Aug. 16, 1996)

ABSTRACT

Time-resolved infrared (IR) radiometry was used to measure surface temperatures during pulsed Er:YSGG (λ=2.79 μm) and Er:YAG (λ=2.94 μm) laser irradiation of dental enamel. Scanning electron microscopy (SEM) was used to determine the melting and vaporization thresholds and to characterize other changes in the surface morphology. The magnitude and temporal evolution of the surface temperature during multiple-pulse irradiation of the tissue was dependent on the wavelength, fluence, and pre-exposure to laser pulses. Radiometry and SEM micrographs indicate that ablation is initiated at temperatures well below the melting and vaporization temperatures of the carbonated hydroxyapatite mineral component (1200 °C). Ablation occurred at lower surface temperatures and at lower fluences for Er:YAG than for Er:YSGG laser irradiation: 400 °C vs. 800 °C and above 7 J/cm^2 vs. 18 J/cm^2, respectively. However, the measured surface temperatures were higher at λ=2.79 μm than at λ=2.94 μm during low fluence irradiation (<7 J/cm^2). Spatially dependent absorption in the enamel matrix is proposed to explain this apparent contradiction.

Keywords dental enamel; Er:YAG laser irradiation; Er:YSGG laser irradiation; laser ablation; radiometry; surface temperature.

1 INTRODUCTION

Since the pioneering work of Stern, Sognnaes and Goodman[1,2] in the 1960s, the potential of lasers for the modification and selective removal of hard dental tissue has been investigated. Hibst and Keller[3–5] have demonstrated that the Er:YAG (λ=2.94 μm) laser can ablate dental hard tissue with efficiencies exceeding those previously reported for other laser wavelengths. Altshuler, Belikov, and Erofeev[6] showed that the Er:YSGG (λ=2.79 μm) laser also ablates hard tissue with high efficiency. It is the generally accepted hypothesis that the subsurface expansion of water is the primary mechanism responsible for exfoliation or spallation of the enamel mineral at temperatures below the melting point of the tissue (~1200 °C) during irradiation near λ=3 μm.[3,4,7–13] In contrast, at the highly absorbed CO_2 laser wavelengths of λ=9.3 and 9.6 μm, the enamel is heated to temperatures above the melting point of carbonated hydroxyapatite (CAP), the mineral component of dental hard tissue before the onset of ablation.[14–23] A lower ablation temperature may be advantageous because the subsequent heat transfer to the interior of the tooth during tissue removal is minimized, thus reducing the risk of pulpal overheating.

At lower fluences below the ablation threshold, IR lasers can also be used for caries preventive treatments. Recent studies by our group have shown that both Er:YAG and Er:YSGG laser radiation can be used to inhibit the progression of artificial carieslike lesions.[24] Studies using CO_2 laser radiation suggest that the enamel surface should be heated to temperatures in excess of 400 to 600 °C in order for preventive treatments to be effective.[17,19,20,25–27]

Knowledge of the surface temperatures during pulsed laser irradiation of enamel is essential for elucidating the mechanism of ablation and the kinetics of the tissue changes occurring during irradiation. Therefore, the aim of this study was to measure the surface temperature of enamel during

Address all correspondence to Daniel Fried. E-mail: dfried@itsa.ucsf.edu

1083-3668/96/$6.00 © 1996 SPIE

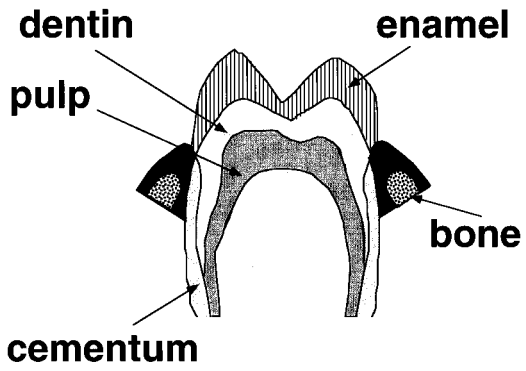

Fig. 1 Cross section of the tooth showing the relative position of the enamel, dentin, cementum, and pulp.

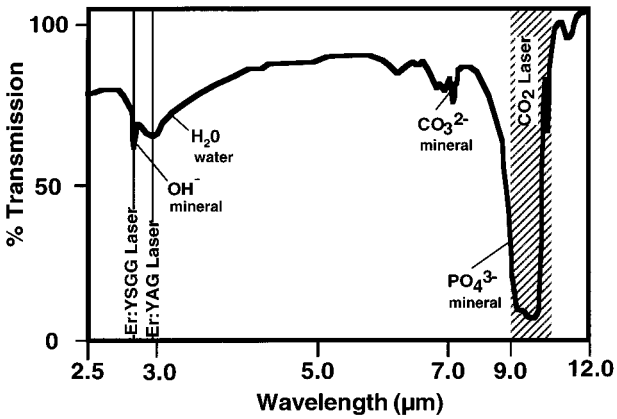

Fig. 2 IR transmission spectrum of carbonated hydroxyapatite (<1%) in a compacted KBr pellet. The laser wavelengths and absorbing species are indicated. The H_2O corresponds to the OH stretch of water incorporated in the enamel matrix, while the source of the (OH^-) band is the OH stretch of the carbonated hydroxyapatite mineral.

Er:YAG and Er:YSGG laser irradiation under various irradiation conditions.

Dental enamel is 85% by volume carbonated hydroxyapatite (50% in dentin and 40% in bone) with 12% water and 3% protein and lipid.[28] The mineral is oriented in hexagonal prisms roughly 4 μm in diameter radiating outward normal to the enamel surface from the dentin-enamel junction (Figure 1). Approximately 25% of the water in enamel and almost all the protein and lipid are located in the interprismatic spaces located between the prisms.[29] The greater part of the water (~75%) in enamel is incorporated as a hydration shell surrounding individual CAP crystals.[29]

All the components of enamel, including mineral, water, protein, and lipid, absorb near λ=3 μm. CAP has a strong absorption maximum near λ=2.8 μm due to the (OH) symmetric stretch and a broad absorption band centered near λ=3 μm due to absorbed water in the interprismatic microspaces of enamel and the waters of hydration that are tightly bound to the mineral. An IR transmission spectrum of carbonated hydroxyapatite powder (<1%) in a compacted KBr pellet (Figure 2) shows that the absorption by the sharp (OH) band of the mineral at λ=2.8 μm may be more significant than the absorption by the intrinsic water at the same wavelength. Er:YSGG laser emission is coincident with this narrow (OH) absorption band while Er:YAG emission overlaps the broad water absorption centered at λ=3 μm. Water is likely to play the principal role in absorption and ablation near λ=3 μm.[28,30]

The absorption coefficient of water is 12,800 cm^{-1} at λ=2.94 μm and 5160 cm^{-1} at λ=2.79 μm.[31] The contribution of the intrinsic water in enamel (interprismatic and waters of hydration) to the overall absorption coefficient, based on the vol. % of water and assuming that the water is uniformly distributed in the enamel matrix, is ~1500 and 620 cm^{-1} at λ=2.94 and 2.79 μm, respectively. Added to the water absorption are the contributions of the (OH) stretch in the mineral centered at λ=2.8 μm and the small organic fraction (protein and lipid). The protein and lipid components absorb near λ=3 μm; however, the percentage of these components is very small and probably has little effect on the absorptive properties of enamel near 3 μm. Protein and lipid may be more influential during the ablation of dentin, cementum, and bone, which have much higher concentrations of protein—approximately 33% by volume (Figure 1).

Caries ablation and preventive treatments typically require multiple pulse irradiation. The absorptive properties of the tissue change as a result of irradiation, influencing the thermal response of subsequent laser pulses incident on the same area of the tooth. Absorbed water is depleted, and chemical changes occur in enamel at temperatures above >100 °C, which may influence the absorption characteristics of subsequent laser pulses.[32–34] Modification of the surface morphology may also influence the thermal response. Previous radiometric measurements during multiple-pulse CO_2 laser irradiation at fluences above the melting threshold showed that there were permanent changes in the thermal response of the tissue for subsequent laser pulses.[15,16,35,36] These changes occurred during the first few laser pulses incident on the same area and the thermal response eventually stabilized after 10 to 50 laser pulses. Similar changes in the thermal response were observed in this study after Er:YAG and Er:YSGG laser irradiation.

As mentioned above, water is assumed to be the primary absorber in enamel near λ=3 μm, therefore the degree of sample hydration is expected to influence the energy deposition and thermal response of enamel during multiple pulse irradiation. Water is also used as a coolant and can interfere with energy deposition. It is the water near the surface that can

be absorbed and desorbed in the ambient environment that is expected to be lost during sample dehydration. The bulk of the water that is incorporated in the enamel crystals requires temperatures in excess of 200 to 300 °C for desorption.[32] In this paper, the changes in the thermal response of hydrated and dehydrated enamel, and enamel with external water applied to the surface water during multiple-pulse-irradiation, are reported for up to 50 incident laser pulses.

SEM micrographs were used to determine ablation thresholds and detect melting and sintering. They greatly facilitate interpretation of the radiometric signals and provide useful insight regarding the mechanism of ablation. SEM micrographs of the area surrounding the Er:YAG laser-irradiated surfaces show ablation without melting the mineral (800 to 1280 °C).[3] In contrast, ablation at the highly absorbed CO_2 laser irradiation wavelengths with similar pulse durations leave a melted, fused, and recrystallized surface.[37] Enamel crystals increase in size at temperatures above 800 °C during slow heating, due to sintering. An increase in the grain size of the crystals can be resolved at a magnification of 60,000 times.[23] SEM studies after CO_2 laser irradiation showed that the crystallite grain size increased by an order of magnitude or larger (40 to 400 nm) after being heated above the melting point.[23,37] The crystal grain size can thus serve as an indication of melting and recrystallization and a surface temperature that exceeded 1200 °C.

The magnitude of the specular and diffuse reflectance at λ=2.79- and 2.94-μm wavelengths were measured in this study to quantify the energy absorption. The reflectivity (specular reflectance) of crystalline materials can increase markedly and approach 100% in regions of strong absorption.[38] The reflectivity of dental enamel rises to above 50% near the λ=9.6-μm resonance of the phosphate ion that is intrinsic to carbonated hydroxyapatite mineral (Figure 2).[14,39,40] Similar increases in the reflectivity, however, were not observed near resonance to the hydroxyl absorption bands of carbonated hydroxyapatite (λ=2.79 μm) and water (λ=2.94 μm) in this study.

2 MATERIALS AND METHODS

2.1 SAMPLE PREPARATION

Plano-parallel sections approximately 1 to 2 mm thick were cut from extracted, unerupted human third molars and incisors. The enamel surfaces were highly polished using a progressively smaller series of 6-, 3-, and 1-μm grit diamond-impregnated disks. The surfaces were rinsed and sonicated in de-ionized water after each polishing step to remove the smear layer and loose debris. Samples were stored in a humid environment and each surface was allowed to dry for approximately 15 min before irradiation to ensure that the surface was dry while the underlying enamel layers were hydrated. Dehydrated samples were prepared to determine the influence of hydration on the thermal response of irradiated samples by leaving them exposed for 48 h, which was sufficient to dehydrate the 2-mm slabs of enamel. The diffusion coefficient (κ) for water in enamel is approximately 1×10^{-8} cm^2/s[41,42]; therefore the time constant for water diffusion in a z=2-mm sample $(z)^2/4(\kappa)$ is ~8–9 h.

2.2 IR RADIOMETRY

The thermal emission from the surface of the enamel was measured during irradiation by either Er:YAG or Er:YSGG lasers (Schwartz Electro-optics Model 1-2-3) at fluences of 1 to 50 J/cm^2. The thermal emission was measured during single- and multiple-pulse irradiation (1 to 50 pulses) incident upon the same area of the sample at a repetition rate of 1 Hz to avoid cumulative heating effects. The free-running erbium lasers produce a pulse train of several micropulses (~1-μs duration) in a macropulse of ~250-μs duration [150 μs full-width half maximum (FWHM)]. The laser energy was measured and calibrated using laser calorimeters, and the laser spot size was measured by scanning a 50-μm diameter pinhole through the beam.

The laser beam was focused to a spot size ~500 μm in diameter (FWHM) on the sample surface. The irradiated surface was aligned at the first focus, f_1 (Figure 3) of a rhodium-coated, ellipsoidal reflector, and the emitted thermal radiation was collected by a thermoelectrically cooled HgCdZnTe (HCZT) detector (BSA Technology Model PCI-L-2TE-12, Torrance, California) placed at the second focus, f_2, of the ellipse. The detector had a response time of ~1 μs and an active area of 1 mm in diameter. The configuration permitted collection of 70% of the thermal emission in a 2π hemisphere above the flat sample (30% is lost through the entrance port of the ellipse). A bandpass filter, λ=3.5 to 9 μm (Spectragon# LP-3500-F) was used to prevent scattered laser radiation from reaching the detector (Figure 3). Laser light reflected from the sample was specularly reflected out the entrance port of the ellipse and was not absorbed by the filter in front of the detector and did not contribute to the detected signal. The detector signal was amplified and digitized using a 500-MHz digital storage oscilloscope (Tektronix 2440) and subsequently transferred to a personal computer for analysis.

The measured signal at the detector (detector volts) was compared with calculated values of the irradiance (W/cm^2) on the detector window to yield the surface temperature. The irradiance on the detector was calculated from the radiant excitance of the (1 mm) area of irradiated enamel using Planck's radiation law assuming blackbody properties and that the surface was a Lambertian radiator. Planck's radiation law was integrated over 0.2-μm spectral intervals in the 3.5 to 9.0-μm IR region and each spectral band was weighted by the transmis-

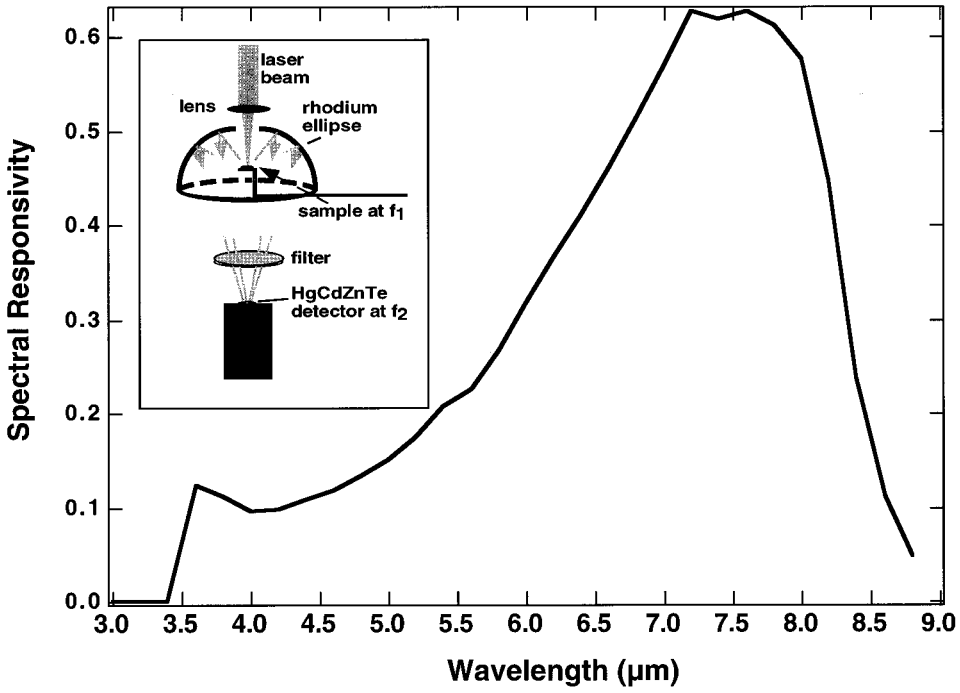

Fig. 3 Product of the responsivity of the detector and the transmission of the 3.5- to 9.0-μm bandpass filter is plotted versus wavelength. The radiometry setup with a rhodium ellipse that collects 70% of the emitted thermal radiation from the irradiated surface and the HgCdZnTe detector (1-μs response time) is shown in the inset to this figure.

sion of the collection optics and the bandpass filter, in addition to the relative spectral responsivity of the detector. The sum of these bands between 3.5 and 9.0 μm and geometrical considerations yielded the expected irradiance on the surface of the detector for each temperature. A lookup table was generated for temperatures from 25 to 4000 °C and used to convert from measured detector volts to temperature.

IR transmission and reflectance spectra indicate that enamel is highly opaque throughout the mid-IR (λ=3.5 to 9 μm), which implies that the emissivity should be high (near blackbody) in this wavelength interval and that the above assumptions are valid. However, it is possible that the emissivity may be lower for the high thermal gradients present during microsecond irradiation;* thus the magnitude of the surface temperatures may be underestimated.[43] Spatial nonuniformity in the laser spot profile can also lead to error; however, the poor imaging quality of the elliptical mirror reduces the contribution of hot spots by smoothing over such spatial inhomogeneities. Similar temperature measurements[36] were performed previously for various irradiation intensities at the highly absorbed CO_2 wavelengths of λ=9.3 and 9.6 μm, at which a surface melt is produced that is clearly discernible with SEM. The fluence thresholds that produced observable surface melting agreed reasonably well with the fluence values that produced single-pulse peak surface temperature excursions near 1200 °C (the melting point of enamel), indicating that the measured temperatures are reasonably accurate.

*The laser energy is deposited in a layer a few microns thick. Accurate determination of the emissivity entails measurement of the transmission through a micron-thick section of enamel throughout the IR, which is not possible with existing sectioning technology. We have measured the IR thermal emission from a synthetic carbonated apatite pellet several millimeters thick placed in a furnace and heated slowly (in thermal equilibrium) from 0 to 1000 °C.[16] The agreement with the computed temperatures was excellent, indicating near blackbody emission. However, the environment of the furnace differs from that during pulsed laser heating because the emissivity depends on the sample thickness.

2.3 SCANNING ELECTRON MICROSCOPY (SEM)

After irradiation, the enamel samples were coated with a layer of gold palladium ~10 nm thick, and observed at 50 to 60,000 times magnification in an SEM (JEOL 820).

2.4 REFLECTANCE MEASUREMENTS

The total reflectance (specular and diffuse) of each sample was measured at low incident fluences (<1 J/cm^2) using a 4-inch diameter gold-coated integrating sphere (Infragold™; coating reflectance >0.97 at λ=3 μm; Labsphere, North Sutton, New Hampshire). A similarly coated port was used as a

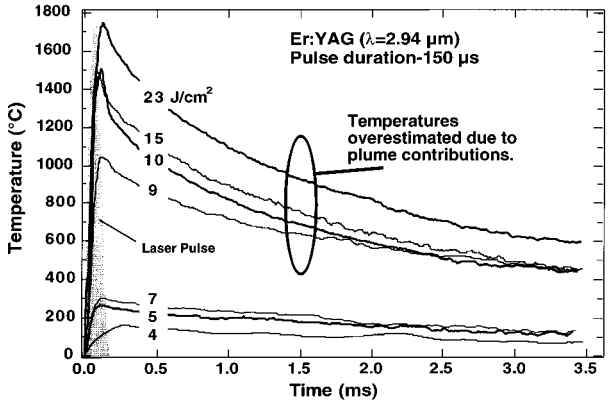

Fig. 4 Typical time-resolved surface temperature profiles during Er:YAG laser irradiation (λ=2.94 μm) of enamel for fluences of 4 to 23 J/cm^2 single pulse. The laser pulse is represented by the shaded area between 0 and 250 μs. The temperatures at or above 9 J/cm^2 are not accurate due to contributions from thermal emission from the plume.

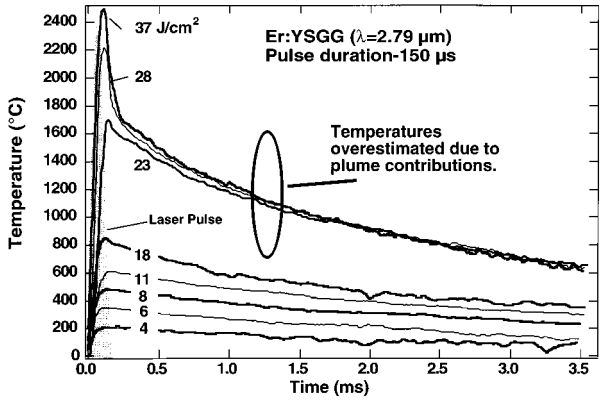

Fig. 5 Typical time-resolved surface temperature profiles during Er:YSGG laser irradiation (λ=2.79 μm) of enamel for fluences of 4 to 37 J/cm^2 single pulse. The laser pulse is represented by the shaded area between 0 and 250 μs. The temperatures at or above 23 J/cm^2 are not accurate due to contributions from thermal emission from the plume.

reflectance standard. An HgCdZnTe detector was placed at the detector port with a baffle placed between this port and the sample.

3 RESULTS

3.1 REFLECTANCE

The sum of the diffuse and specular of enamel at λ=2.79 and 2.94 μm was relatively low, 5±2% and 5±1% (mean±SD, n=10), respectively. These data indicate that the reflectivity of enamel in this region does not increase significantly near the (OH) and (H_2O) resonances in the mineral. The low reflectance also indicates that scattering does not significantly influence energy deposition. In contrast, in the UV, visible, and near-IR regions, scattering greatly influences the deposition of the laser energy in dental hard tissues.[44,45]

3.2 SURFACE TEMPERATURE MEASUREMENTS

3.2.1 Er:YAG Laser Irradiation

The surface temperatures during Er:YAG laser irradiation for various incident fluences are shown in Figure 4. At irradiation fluences below 9 J/cm^2, the peak temperature increased monotonically with the applied fluence. There was a marked increase in the emitted thermal radiation (apparent temperature) at 350 °C to over 1000 °C when the fluence was raised from 7 to 9 J/cm^2. Above 9 J/cm^2, the peak surface temperature no longer exhibited a simple dependence on the incident fluence. SEM micrographs show an etched surface, indicating that material is removed at fluences greater than 7 J/cm^2. The large increase in the thermal radiation signal at ablative fluences is most easily attributed to thermal emissions originating from ejected mineral in the field of view of the radiometer. It was not possible to differentiate between the thermal emission originating from the ejected particles and the surface. Therefore, above 7 to 9 J/cm^2, the surface temperatures are most likely overestimated. Qualitatively, the thermal radiation signal is useful for further analysis, but the temperature scales shown are no longer applicable after the onset of ablation.

3.2.2 Er:YSGG Laser Irradiation

A similar trend in surface temperatures was observed with increasing fluence for the Er:YSGG laser series, with some notable differences (Figure 5). The large increase in thermal emission at the ablation threshold occurred at a higher fluence (>18 J/cm^2) and at a higher surface temperature (800 °C). At lower fluences, peak surface temperatures were ~30% higher for Er:YSGG than for Er:YAG laser irradiation.

There are sharp excursions in the thermal emission that were present only during the first 200 μs, for fluences above the ablation threshold (>18 J/cm^2). These sharp temperature excursions in the thermal emission are characteristic of emission from the plume of gases and small particles ejected from the irradiated area. Such isolated particles can be heated to very high temperatures because they are thermally isolated from the sample and cannot cool via heat conduction. The temporal evolution of the plume emission coincided with the intensity variation of the incident laser pulse, indicating that the particles in the plume were absorbing the incident laser radiation and emitting thermal radiation at similar rates (i.e., in apparent radiative equilibrium). This feature was not as distinct during Er:YAG laser irradiation (Figure 4) as it was for the Er:YSGG and during CO_2 irradiation where the mineral absorbs in the vapor phase.[15,16,36]

At ablative fluences, the apparent temperatures at later times after the sharp peak in the surface temperature (t>250 μs) has subsided are expected to be more representative of the surface temperature and contain smaller contributions of thermal emission from the plume. Thermal emission from the plume is expected to quickly subside due to the rapid expansion of the plume outside the field of view of the detector and the accelerated radiative cooling rates of the small particles in the plume because of the increased emitting area. However, slow-moving large particles may still contribute significantly to the measured thermal emission for several milliseconds after the laser pulse for fluences above the ablation threshold. Moreover, the increased surface roughness of the ablated area may increase the effective thermal relaxation time and reduce the rate of fall off of the surface temperature. These accumulated effects may lead to an overestimation of the surface temperature. Therefore accurate temperatures for fluences above the ablation threshold cannot be calculated from the thermal emission, even for later times after the bright plume has subsided >250 μs. Although the thermal emission at fluences above the ablation threshold does not accurately reflect either the temperature of the enamel surface or the plume, the temporal evolution of the thermal emission is qualitatively useful for understanding the changes in the ablation dynamics and the energy coupling to the enamel surface during multiple-pulse irradiation.

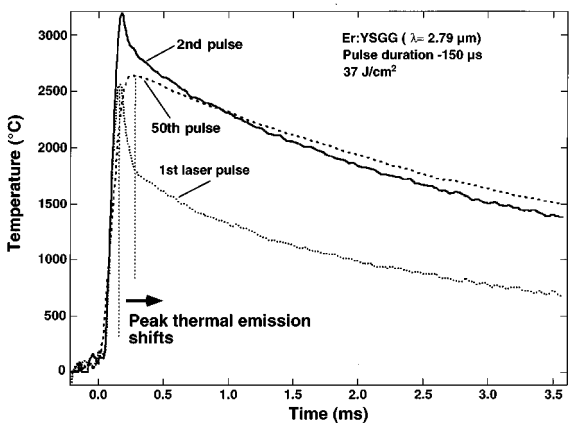

Fig. 6 Thermal emission during multiple-pulse Er:YSGG laser irradiation (λ=2.79 μm) of enamel. The repetition rate was 1 Hz to avoid cumulative heating effects. The fluence was 37 J/cm^2 and the pulse duration was 150 μs. The thermal emission from the first pulse contains two components of thermal emission: the first component, the plume emission, peaks near the FWHM of the laser pulse at 150 μs and the second component, emission from the surface, peaks at the end of the 250-μs laser pulse. The thermal emission after the fiftieth pulse peaks at 250 μs and contains mostly emission from the sample surface.

3.3 CHANGES IN PHOTOTHERMAL RESPONSE DUE TO MULTIPLE-PULSE IRRADIATION

For fluences above the ablation threshold, the thermal response changed markedly for subsequent laser pulses incident on the same area of the sample at both erbium wavelengths. A typical sequence of the pulse-dependent thermal response of enamel is shown in Figure 6 during Er:YSGG laser irradiation at 37 J/cm^2. The thermal emission profiles for the first few pulses contain the characteristic sharp spike that was evident in Figure 5, which is associated with thermal emission from the laser-heated plume present during the laser pulse. The sharp peak in thermal emission typically changed markedly during the first few pulses, with the maximum emission after the second to fifth laser pulse. The sharp peak subsequently decreased in amplitude after the first few laser pulses and disappeared by the tenth to fiftieth pulse, and the thermal emission from the sample "stabilized" with minimal changes in the thermal profiles for subsequent laser pulses (Figure 6). There was normally a loud, audible snap associated with the first few laser pulses. Such a sound typically indicates the explosive release of gases accompanied by the production of a strong acoustic wave in air. The snap was notably weaker for the second and third pulses and was no longer audible after several laser pulses, suggesting less energetic expansion of the ablated material.

The thermal emission at later times, after the incident laser pulse (t>250 μs), which is more representative of thermal emission from the enamel surface, rose with increasing number of laser pulses, in contrast to the thermal emission during the first 250 μs, which is more representative of plume emission. This rise in the thermal emission from the surface (t>250 μs) after the first "ablative laser pulses" reflects increased energy coupling to the sample, with less kinetic and internal energy imparted to the ablated material.

The peak of the thermal emission from the sample during the first laser pulse coincided with the peak intensity of the laser emission (t=150 μs), while the peak of the thermal emission during the fiftieth laser pulse coincided with the end of the laser pulse (t=250 μs, Figure 6). Assuming an absorption coefficient in the range of 300 to 1500 cm^{-1}, the thermal relaxation time (heat conduction) of the heated layer of the enamel surface is ~100 to 1000 μs (τ_z=1/4 $\mu^2\kappa$).[46] With thermal relaxation times in the hundreds of microseconds range, the peak surface temperature should occur at the end of the laser pulse and not at the peak intensity of the incident laser pulse. Therefore, the temporal shift in the peak of thermal emission, the decrease in the initial sharp peak representing plume emission, and the corresponding rise in the thermal emission at later times are all consistent with a shift of emphasis

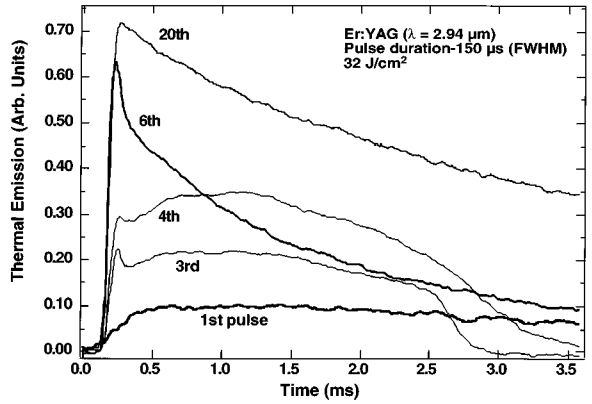

Fig. 7 Thermal emission during multiple pulse Er:YAG laser (λ =2.94 μm) irradiation of enamel after a drop of water of ~500 μm thickness was applied to the surface. The repetition rate was 1 Hz to avoid cumulative heating effects. The fluence was 32 J/cm^2 and the pulse duration was 150 μs. The unusual temporal evolution of this signal was caused by water shielding the enamel surface. The thermal emission could only be detected after the recoil pressure from the vaporization of the surface water displaced the water from the irradiated area. The water rebounded after a few milliseconds, covering the enamel surface and terminating the thermal emission. After the sixth pulse, all the water had been removed and the subsequent emission profiles resembled those of the dry surface (Fig. 6).

from thermal emission by the plume to thermal emission from the sample surface with increasing number of laser pulses.

3.4 INFLUENCE OF SAMPLE HYDRATION ON THERMAL RESPONSE

There were no measurable differences in the surface temperature profiles acquired for samples after the nominal 15-min exposure to dry the outer surface and for the more extensively dehydrated samples.

The influence of externally applied water (droplet applied to surface) on the thermal response of irradiated enamel was also investigated. Surface temperatures measured at a fluence of 32 J/cm^2 for the first through twentieth pulses of the Er:YAG laser are shown in Figure 7. The response for the first few pulses was markedly different than those of Figure 6. The first few pulses have a distinctive shape, peaking well after the end of the laser pulse. Cavitation experiments in water during laser irradiation have shown that the first few micropulses of the laser macropulse displace the water around the laser spot, causing a cavity.[47–49] It is likely that a similar mechanism applies in this situation (i.e., the recoil forces due to water vaporization displace the water from the irradiated area). As a reviewer of this paper has suggested, bleaching of the λ=3 μm water absorption band may enable radiation to penetrate the water layer and heat the enamel surface.[31] Water (liquid phase) absorbs the thermal emission from the enamel surface in the range of λ=3.5 to 9 μm; therefore, we must be observing thermal emission from the enamel surface after the layer of water has been displaced or evaporated from the irradiated area. Water vapor does not absorb at 2.94 μm so it probably does not interfere with the incident laser pulse.

The first laser pulses failed to displace the water layer, and the magnitude of the thermal emission was very low. During the third and fourth laser pulses, there is a sharp temperature rise after 200 μs, which is typical of ablation on dry samples and indicates that more surface water is displaced from the laser spot. During the third and fourth laser pulses, the thermal emission drops abruptly after 2.5 ms. The water layer that was initially displaced by the recoil forces of the vaporized water has returned to cover the exposed laser spot, abruptly cutting off the thermal radiation from the surface. The temporal evolution of the expansion (~1 ms) and collapse (~2 to 3 ms) of the displaced water for the third and fourth pulses scales approximately with the temporal evolution of cavitation bubbles in water for similar laser pulses.[47–49] After the water layer was removed, a progression similar to that of Figure 6 was observed, and the sixth and twentieth pulses of Figure 7 resembled the thermal response of the second and fiftieth pulses, which were acquired on dry surfaces (Figure 6). Similar sequences were observed for λ=2.79 μm laser radiation incident on enamel with water applied to the surface.

3.5 SCANNING ELECTRON MICROGRAPHS

There was no evidence of surface melting or sintering around the zone of ablation after Er:YAG irradiation at fluences of less than 32 J/cm^2 [Figure 8(b)]. The enamel crystals were unchanged by irradiation. In contrast, after Er:YSGG laser irradiation above 27 J/cm^2 [Figure 8(a)], there was noticeable sintering of the enamel crystals with almost complete fusion of the crystals above 50 J/cm^2 [Figure 9(a)]. Micrographs obtained at higher magnification (60,000×) clearly show that the individual enamel crystals, normally 40 nm in diameter, have fused together to form crystals at least an order of magnitude larger [Figure 9(b)].

4 DISCUSSION

4.1 SURFACE TEMPERATURE MEASUREMENTS

Er:YAG and Er:YSGG laser irradiation of dental enamel at fluences below the ablation thresholds of 7 and 18 J/cm^2, respectively, does not induce detectable changes in the enamel, and further surface temperatures are reproducible from pulse to pulse. Surface temperature excursions produced at fluences less than 7 J/cm^2 are 30% higher for Er:YSGG than for Er:YAG laser irradiation (see Figures 4 and 5). This difference in surface temperature is indicative of higher total absorption (H_2O+apatite

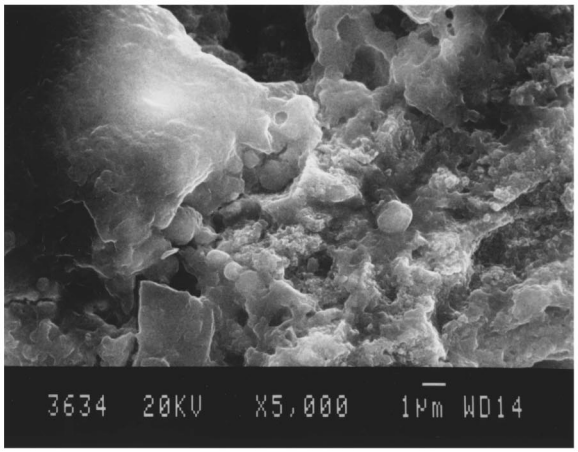

(a)

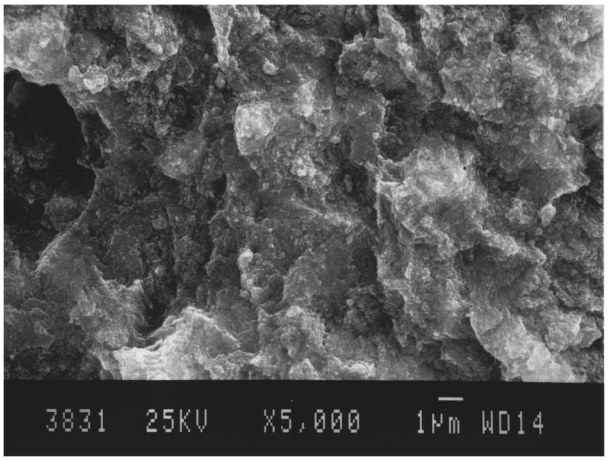

(b)

Fig. 8 Typical SEM micrographs of the interior of the craters created after Er:YSGG (λ=2.79) irradiation at 27 J/cm^2 (a) and Er:YAG (λ=2.94) irradiation at 32 J/cm^2 (b). Melting and fused enamel occur in some areas of the crater in (a), while the surface in (b) is etched with no evidence of melting anywhere in the crater area.

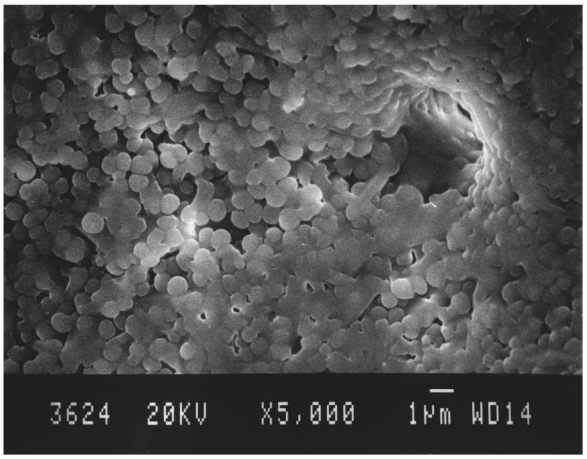

(a)

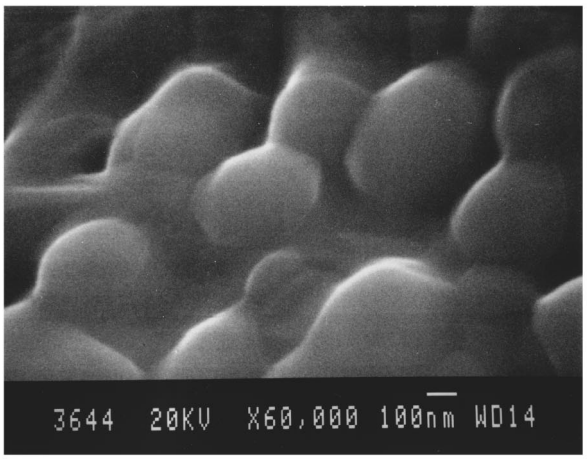

(b)

Fig. 9 Typical SEM micrographs at magnifications of 5000×(a) and 60,000×(b) of the interior of the craters after Er:YSGG (λ =2.79) irradiation at 50 J/cm^2. The enamel crystals have recrystalized after melting to form large single crystals with grain sizes several orders of magnitude larger than the original crystallites.

+protein+lipid) at λ=2.79 μm and suggests that Er:YSGG laser radiation is more highly absorbed by the mineral of dental enamel than Er:YAG laser radiation, even though the ablation threshold is markedly higher.

At higher fluences, above the respective ablation thresholds, large particles of unmelted mineral were visible near the periphery of the ablation crater, indicating that intact material was ejected from the sample. The early part of the radiometry/temperature profiles during high-intensity irradiation by the Er:YSGG laser pulses manifests a sharp peak in temperature due to plume emission that increases with increasing fluence and follows the temporal evolution of the laser pulse. This plume emission, which arises from absorption of the incident laser radiation by particles and vapor in the plume, is not as prominent during irradiation at λ=2.94 μm (Figure 4). Since water vapor is transparent to λ=2.94 and 2.79 μm laser radiation, only the mineral component in the plume is expected to absorb a significant fraction of the incident laser radiation.[31] The mineral absorbs strongly at λ=2.79 μm due to the (OH) in hydroxyapatite; in contrast, the λ=2.94-μm wavelength is only weakly absorbed by the mineral phase. Therefore fragments of solid mineral and liquid–vapor phase mineral in the plume are expected to be heated to higher temperatures by λ=2.79 μm than by λ=2.94 μm laser radiation. At CO_2 laser wavelengths, the laser radiation is more strongly absorbed by the mineral component of enamel, and these sharp temperature excursions due to thermal emission from plume vapor are even more prominent during multiple-pulse CO_2 laser irradiation at ablative fluences.[15,16,36] Since Er:YSGG laser radiation is more strongly absorbed by the mineral phase of enamel than water, the time-resolved temperature profiles more closely

resembled those measured at CO_2 laser wavelengths than at λ=2.94 μm.[36,50]

The thermal emission measured at later times after the plume emission has subsided (t>250 μs) is dominated by the thermal emission from the enamel surface. Thus, the thermal emission at later times is more representative of the actual temperature of the surface and the laser energy that remains in the enamel surface after the ablation event, albeit the temperature may be overestimated due to some thermal emission from slow-moving particles that do not leave the field of view of the detector, and changes in the enamel surface morphology that affect the thermal diffusivity. Corresponding changes in the temporal evolution and magnitude of the surface temperatures during multiple-pulse irradiation at ablative fluences reflect changes in the amount of laser energy that is coupled to the plume, imparted to the ablated material, and deposited in the sample.[15,32,50]

Accounting for the redistribution of the absorbed energy is fundamental to understanding the mechanism of ablation and minimizing the heat deposition in the tooth during ablation. The risk of excessive heat deposition in the tooth is one of the principal factors that must be overcome before lasers can be used safely for cavity preparations in dentistry. The observation that the measured thermal profiles stabilize after the plume emission disappears indicates that energy is no longer taken away by the ablation products. Therefore a reduction in the magnitude of plume emission reflects variations in the quantity of material ejected and a decrease in the ablation rate during multiple-pulse irradiation at the erbium laser wavelengths used in this study. For moderate ablative fluences, plume production is present during the first few laser pulses; thereafter ablation effectively stalls and plume emission ceases. At higher fluences, ablation continues without stalling and after 50 laser pulses there is still significant plume emission. A similar progression of events was noted for irradiation at CO_2 wavelengths.[36]

The large increase in the coupling of energy to the tooth for increasing number of laser pulses is a manifestation of laser-induced changes in the surface morphology and the composition of the irradiated enamel that effectively retard the ablation efficiency. During multiple-pulse Er:YAG laser irradiation of enamel and bone, there is an apparent decrease in the ablation rate which has been ascribed to tissue desiccation.[10,51,52] Assuming that ablation of enamel occurs subsequent to rapid heating and the explosive expansion of the water within the crystalline lattice of enamel, if the intrinsic water peripheral to the ablation site is lost due to repeated temperature excursions exceeding 300 °C, then the ablation efficiency and plume production will decrease as the number of delivered laser pulses increases.

4.2 INFLUENCE OF HYDRATION AND AN ADDED WATER LAYER

There were no significant changes in the measured surface temperature profiles of enamel samples that were allowed to dry for 15 min and 48 h. These results imply that weakly bound or absorbed water that can readily evaporate in the ambient atmosphere does not significantly influence the absorption of λ=3 μm laser radiation. Thermal analysis indicates that most of the water in enamel is tightly bound to the mineral lattice and that temperatures much greater than the vaporization temperature of water (100 °C at 1 atm) are required to remove it.[32] Analysis of the intensity of the λ=3 μm water band of tooth enamel heated in a tube furnace (dry N_2 atmosphere) using IR spectroscopy shows that one-third of the water in enamel is lost between 25 and 270 °C, another third is lost between 270 and 300 °C, and the remaining water is lost by 900 °C.[32] Similar studies showed that two-thirds of the water and carbonate are lost after heating in a tube furnace to 650 °C and after laser heating using a cw CO_2 laser.[33,34]

The addition of a water layer to the sample surface greatly perturbed the measured thermal profiles. However, the laser energy was able to penetrate the water layer and heat the enamel surface. After the first few pulses, the absorbed water had evaporated and no longer influenced the thermal response of the irradiated tissue. These data suggest that the use of water as coolant at λ=3 μm should only reduce the effective ablation rate. Certainly, the application of water and air cooling before and after or between a series of laser pulses will serve to reduce the risk of pulpal overheating. However, there is some question about the effectiveness of simultaneous water cooling during the irradiation of dental hard tissue since more energy will be required to remove the same amount of tissue.

4.3 SPATIALLY DEPENDENT ABSORPTION

The threshold for ablation is markedly lower for Er:YAG laser radiation (7 J/cm^2) than for Er:YSGG laser radiation (18 J/cm^2), with corresponding surface temperatures of 300 and 800 °C. The surface temperature of enamel during laser irradiation at fluences below the ablation threshold indicated that Er:YSGG laser radiation heated the enamel surface to temperatures ~30% higher for similar fluences than for Er:YAG laser radiation. These results are in apparent contradiction because one expects a lower ablation threshold for the more highly absorbed radiation. However, if ablation is due to stress-induced exfoliation and spallation by the explosive release of subsurface gases, then this apparent contradiction is more understandable. Higher measured surface temperatures for Er:YSGG over Er:YAG laser irradiation and lower ablation thresholds for the Er:YAG laser radiation may re-

sult from variation of the absorption coefficient with distance from the enamel surface. There is some evidence that the water in enamel varies in concentration with distance from the surface. Sowa and Mantsch[53] used step-scan photoacoustic Fourier transform infrared spectroscopy (FTIR) to depth profile the broad λ=3 μm absorption band for water in enamel. The concentration of water increased significantly with increased sampling depth. In addition, IR spectra of the enamel surface acquired in our laboratory using specular reflectance FTIR, a method that samples only the outer few microns of the enamel surface, lack the broad water absorption band centered at λ=3 μm. These spectra, acquired using separate FTIR methods, suggest that the water content of enamel increases with depth from the surface and that water is absent from the outer few micrometers. If the outer few microns of the enamel surface have relatively little water, then the absorption in the enamel will be spatially dependent.

A plausible explanation for the observed results is based on the assumption that the outer few microns of the enamel contain a gradient in water content, with the water content increasing with distance from the surface. Er:YSGG laser radiation, which is directly absorbed by the (OH) of the carbonated hydroxyapatite mineral, will be more highly absorbed in the outer water-deficient layer than Er:YAG laser radiation, which is primarily absorbed by water. Only thermal radiation originating from the outer few microns of enamel is detected by our radiometry system; hence our measurements detect higher surface temperatures for the Er:YSGG than for the Er:YAG laser irradiation for similar fluences.

Laser radiation that penetrates the outer water-deficient layer and heat conducted from the surface may raise the subsurface water to temperatures exceeding the boiling point. The inertially confined water can create great subsurface stresses, leading to explosive removal of the outer layers of enamel.[54] Since more λ=2.94 μm laser radiation is expected to be transmitted through the outer few microns of the primarily mineral, water-deficient enamel, this wavelength is more highly absorbed by the subsurface water than λ=2.79 μm radiation. It is likely that steeper temperature gradients and correspondingly greater stresses will be induced in the tissue, leading to lower exfoliating and ablating temperatures for Er:YAG than for Er:YSGG laser irradiation. This absorption mechanism provides a likely explanation for the apparent contradiction between higher surface temperatures and higher ablation thresholds measured for the Er:YSGG and the Er:YAG lasers. However, additional experiments and detailed model calculations are necessary to confirm this hypothesis.

5 CONCLUSIONS

IR radiometry and SEM observations indicate significant differences in absorption and ablation for Er:YAG and Er:YSGG laser irradiation in enamel. The ablation threshold was markedly lower for Er:YAG than for Er:YSGG laser irradiation. Therefore the Er:YAG may be better suited for the ablative removal of enamel. On the other hand, the surface of enamel can be efficiently heated to higher temperatures using λ=2.79-μm rather than 2.94-μm laser irradiation with 250-μs pulses, before the onset of ablation. Thus, Er:YSGG laser radiation may be better suited for caries preventive treatments that require localized surface heating, as previously reported for other wavelengths.[17,19,20,25–27] In addition, the Er:YSGG laser radiation is more amenable to delivery via optical fiber than Er:YAG (λ=2.94 μm) and CO_2 laser wavelengths (λ=9 to 11 μm).

Acknowledgments

This work was supported by grants from the National Institutes of Health/National Institutes of Dental Research (DE 09958), NIH (GM50534) and the National Science Foundation BES (9222483 and 9257492).

REFERENCES

1. R. H. Stern, R. F. Sognnaes, and F. Goodman, ''Laser effect on *in vitro* enamel permeability and solubility,'' *J. Am. Dent. Assoc.* **78**, 838–843 (1966).
2. R. H. Stern, J. Vahl, and R. F. Sognnaes, ''Ultrastructural observations of pulsed carbon dioxide laser effects,'' *J. Dent. Res.* **51**, 455–460 (1972).
3. U. Keller and R. Hibst, ''Experimental studies of the application of the Er:YAG laser on dental hard substances: II. Light microscopic and SEM investigations,'' *Lasers Surg. Med.* **9**, 345–351 (1989).
4. R. Hibst and U. Keller, ''Experimental studies of the application of the Er:YAG laser on dental hard substances: I. Measurement of the ablation rate,'' *Lasers Surg. Med.* **9**, 338–344 (1989).
5. R. Hibst and U. Keller, ''Heat effect of pulsed Er:YAG laser radiation,'' *Proc. SPIE* **1200**, 379–386 (1990).
6. G. B. Altshuler, A. V. Belikov, and A. V. Erofeev, ''Laser treatment of enamel and dentin by different Er-lasers,'' *Proc. SPIE* **2128**, 273–281 (1994).
7. J. A. Izatt, D. Albagli, I. Itzkan, and M. S. Feld, ''Pulsed laser ablation of calcified tissue: physical mechanisms and fundamental parameters,'' *Proc. SPIE* **1202**, 133–140 (1990).
8. E. N. Sobol, *Phase Transformations and Ablation in Laser-Treated Solids*, Wiley, New York (1995).
9. J. A. Izatt, N. D. Sankey, F. Partovi, M. Fitzmaurice, R. P. Rava, I. Itzkan, and M. S. Feld, ''Ablation of calcified biological tissue using pulsed hydrogen fluoride laser radiation,'' *IEEE J. Quant. Electron.* **26**(12), 2261–2270 (1990).
10. J. T. Walsh and T. F. Deutsch, ''Er:YAG ablation of tissue: Measurement of ablation rates,'' *Lasers Surg. Med.* **9**, 327–337 (1989).
11. J. T. Walsh, Jr. and T. F. Deutsch, ''Measurement of Er:YAG laser ablation plume dynamics,'' *Appl. Phys. B* **52**, 217–224 (1991).
12. V. Romano, R. Rodriguez, H. J. Altermatt, M. Frenz, and H. P. Weber, ''Bone microsurgery with IR-lasers: a comparative study of the thermal action at different wavelengths,'' *Proc. SPIE* **2077**, 87–96 (1994).
13. R. Hibst and U. Keller, ''Mechanism of Er:YAG laser induced ablation of dental hard substances,'' *Proc. SPIE* **1880**, 156–162 (1993).

14. G. Duplain, R. Boulay, and P. A. Belanger, ''Complex index of refraction of dental enamel at CO_2 wavelengths,'' *Appl. Opt.* **26**, 4447–4451 (1987).
15. D. Fried, W. D. Seka, J. D. B. Featherstone, and R. E. Glena, ''Multiple pulse irradiation of dental hard tissues at CO_2 laser wavelengths,'' *Proc. SPIE* **2394**, 41–50 (1995).
16. D. Fried, S. F. Borzillary, S. M. McCormack, R. E. Glena, J. D. B. Featherstone, and W. Seka, ''The thermal effects on CO_2 laser irradiated dental enamel at 9.3, 9.6, 10.3, and 10.6 μm,'' *Proc. SPIE* **2128**, 319–328 (1994).
17. J. D. B. Featherstone and D. G. A. Nelson, ''Laser effects on dental hard tissue,'' *Adv. Dent. Res.* **1**(1), 21–26 (1987).
18. J. D. B. Featherstone, S. H. Zhang, M. Shariati, and S. M. McCormack, ''Carbon dioxide laser effects on caries-like lesions of dental enamel,'' *Proc. SPIE* **1424**, 145–149 (1991).
19. J. D. B. Featherstone, N. A. Barrett-Vespone, D. Fried, Z. Kantorowitz, and J. Lofthouse, ''Rational choice of CO_2 laser conditions for inhibition of caries progression,'' *Proc. SPIE* **2394**, 57–67 (1995).
20. J. D. B. Featherstone, N. A. Barrett-Vespone, D. Fried, Z. Kantorowitz, and J. Lofthouse, ''CO_2 laser inhibition of artificial caries-like lesion progression in dental enamel,'' *J. Dent. Res.* (in press), 1996.
21. D. G. A. Nelson, M. Shariati, R. Glena, C. P. Shields, and J. D. B. Featherstone, ''Effect of pulsed low energy infrared laser irradiation on artificial caries-like lesion formation,'' *Caries Res.* **20**, 289–299 (1986).
22. D. G. A. Nelson, W. L. Jongebloed, and J. D. B. Featherstone, ''Laser irradiation of human dental enamel and dentine,'' *NZ Dent. J.* **82**, 74–77 (1986).
23. D. G. A. Nelson, J. S. Wefel, W. L. Jongebloed, and J. D. B. Featherstone, ''Morphology, histology and crystallography of human dental enamel treated with pulsed low energy IR laser radiation,'' *Caries Res.* **21**, 411–426 (1987).
24. D. Fried, S. R. Visuri, J. D. B. Featherstone, W. Seka, and J. T. Walsh, ''Caries inhibition potential of Er:YAG and ER:YSGG laser radiation,'' *Proc. SPIE* **2672**, 73–78 (1996).
25. J. L. Fox, D. Yu, M. Otsuka, W. I. Higuchi, J. Wong, and G. L. Powell, ''Initial dissolution rate studies on dental enamel after CO_2 laser irradiation,'' *J. Dent. Res.* **71**, 1389–1397 (1992).
26. J. L. Fox, D. Yu, M. Otsuka, W. I. Higuchi, J. Wong, and G. L. Powell, ''The combined effects of laser irradiation and chemical inhibitors on the dissolution of dental enamel,'' *Caries Res.* **26**, 333–339 (1992).
27. J. L. Fox, J. Wong, D. Yu, M. Otsuka, W. I. Higuchi, J. Hsu, and G. L. Powell, ''Carbonate apatite as a model for the effect of laser irradiation on human dental enamel,'' *J. Dent. Res.* **73**(12), 1848–1853 (1994).
28. M. E. J. Curzon and J. D. B. Featherstone, ''Chemical composition of enamel,'' in *Handbook of Experimental Aspects of Oral Biochemistry*, E. P. Lazzan, Ed., pp. 123–135, CRC Press, Boca Raton, FL (1983).
29. R. E. Jordan, L. Abrams, and B. S. Kraus, *Kraus' Dental Anatomy and Occlusion*, Mosby Year Book, New York (1992).
30. F. C. M. Driessens and R. M. H. Verbeeck, Ed., *Biominerals*, CRC Press, Boca Raton, FL (1990).
31. K. L. Vodop'yanov, ''Bleaching of water by intense light at the maximum of the $\lambda \sim 3$ μm absorption band,'' *Sov. Phys. JETP* **70**(1), 114–347 (1990).
32. D. W. Holcomb and R. A. Young, ''Thermal decomposition of human tooth enamel,'' *Calcif. Tissue Int.* **31**, 189–201 (1980).
33. S. Kuroda and B. O. Fowler, ''Compositional, structural and phase changes in *in vitro* laser-irradiated human tooth enamel,'' *Calcif. Tissue Int.* **36**, 361–369 (1984).
34. B. O. Fowler and S. Kuroda, ''Changes in heated and in laser-irradiated human tooth enamel and their probable effects on solubility,'' *Calcif. Tissue Int.* **38**, 197–208 (1986).
35. J. P. Moss, B. C. M. Patel, G. J. Pearson, G. Arthur, and R. A. Lawes, ''Krypton fluoride excimer ablation of tooth tissues: precision tissue machining,'' *Biomaterials* **15**(12), 1013–1018 (1994).
36. D. Fried, W. Seka, R. E. Glena, and J. D. B. Featherstone, ''The thermal response of dental hard tissues to 9–11 μm CO_2 laser irradiation,'' *Opt. Eng.* **35**(7), 1976–1984 (1996).
37. S. M. McCormack, D. Fried, J. D. B. Featherstone, and W. Seka, ''Scanning electron microscope observations of CO_2 laser effects on dental enamel,'' *J. Dent. Res.* **74**(10), 1702–1708 (1996).
38. S. S. Mitra, ''Optical properties of nonmetallic solids for photon energies below the fundamental band gap,'' in *Handbook of Optical Constants of Solids*, E. D. Palik, Ed., pp. 213–269, Academic Press, New York (1985).
39. D. Fried, W. Seka, R. E. Glena, and J. D. B. Featherstone, ''Permanent and transient changes in the reflectance of CO_2 laser irradiated dental hard tissues at λ=9.3, 9.6, 10.3, and 10.6 μm and at fluences of 1–20 J/cm^2,'' *Lasers in Surg. Med.* (in press), 1996.
40. W. D. Seka, D. Fried, J. D. B. Featherstone, and R. E. Glena, ''Time-dependent reflection and surface temperatures during CO_2 laser irradiation of hard dental tissues with 50–500 μs pulses,'' *Proc. SPIE* **2394**, 51–56 (1995).
41. E. J. Burke and E. C. Moreno, ''Diffusion fluxes of tritiated water across human enamel membranes,'' *Arch. Oral Biol.* **20**, 327–332 (1975).
42. G. H. Dibdin, ''The water in human dental enamel and its diffusional exchange measured by clearance of tritiated water from enamel slabs of varying thickness,'' *Caries Res.* **27**, 81–86 (1993).
43. J. W. Valvano and J. Pearce, ''Temperature Measurements,'' in *Optical-Thermal Response of Laser Irradiated Tissue*, A. J. Welch and M. J. C. van Gemert, Eds., pp. 526–528, Plenum, New York (1995).
44. D. Fried, J. D. B. Featherstone, R. E. Glena, and W. Seka, ''The nature of light scattering in dental enamel and dentin at visible and near-IR wavelengths,'' *Appl. Opt.* **34**(7), 1278–1285 (1995).
45. D. Spitzer and J. J. ten Bosch, ''The absorption and scattering of light in bovine and human dental enamel,'' *Calcif. Tiss. Res.* **17**, 129–137 (1975).
46. M. J. C. van Gemert and A. J. Welch, ''Time constants in thermal laser medicine,'' *Lasers Surg. Med.* **9**, 405–421 (1989).
47. C. P. Lin, D. Stern, and C. A. Puliafito, ''High-speed photography of Er:YAG laser ablation in fluid: implication for laser vitreous surgery,'' *Invest. Ophthalmol. Vis. Sci.* **31**(12), 2546–2550 (1990).
48. M. Forrer, M. Ith, M. Frenz, V. Romano, H. P. Weber, A. Silenok, and V. I. Konov, ''Mechanism of channel propagation in water by pulsed erbium laser radiation,'' *Proc. SPIE* **2077**, 104–112 (1993).
49. H. Loertscher, W. Q. Shi, and W. S. Grundfest, ''Tissue ablation through water with erbium:YAG lasers,'' *IEEE Trans. Biomed. Eng.* **39**(1), 86–88 (1992).
50. W. Seka, J. D. B. Featherstone, D. Fried, S. R. Visuri, and J. T. Walsh, ''Laser ablation of dental hard tissue: from explosive ablation to plasma-mediated ablation,'' *Proc. SPIE* **2672**, 144–158 (1996).
51. J. T. Walsh and D. A. Hill, ''Erbium laser ablation of bone: effect of water content,'' *Proc. SPIE* **1427**, 27–33 (1991).
52. V. A. Vickers, S. L. Jacques, J. Schwartz, M. Motamedi, S. Rastegar, and J. W. Martin, ''Ablation of hard dental tissues with the Er:YAG laser,'' *Proc. SPIE* **1646**, 46–55 (1992).
53. M. G. Sowa and H. H. Mantsch, ''FT-IR step-scan photoacoustic phase analysis and depth profiling of calcified tissue,'' *Appl. Spectroscopy* **48**(3), 316–319 (1994).
54. D. Albagli, L. T. Perelman, G. S. Janes, C. von Rosenburg, I. Itzkan, and M. S. Feld, ''Inertially confined ablation of biological tissue,'' *Lasers Life Sci.* **6**(1), 55–68 (1994).